COMPOSITE MATERIAL HOLLOW ANTIRESONANT FIBERS

Walter Belardi*, Francesco De Lucia, Francesco Poletti and Pier J. Sazio

Optoelectronics Research Centre, University of Southampton, Highfield, Southampton, Hampshire. SO17 1BJ, UK
**Corresponding author: w.belardi@soton.ac.uk*

Received XX Month XXXX; revised XX Month, XXXX; accepted XX Month XXXX; posted XX Month XXXX (Doc. ID XXXXX); published XX Month XXXX

We study novel designs of hollow core antiresonant fibers comprising multiple materials in their core boundary membrane. We show that this type of fiber still satisfies an antiresonance condition and compare their properties to those of an ideal single-material fiber with an equivalent thickness and refractive index. As a practical consequence of this concept, we discuss the first realization and characterization of a composite silicon/glass based hollow antiresonant fiber. © 2017 Optical Society of America

OCIS codes: (060.2280) Fiber design and fabrication; *(*060.2400) Fiber properties*;* (060.4005) Microstructured fibers

http://dx.doi.org/10.1364/OL.99.099999

After almost two decades of improvement in fiber technology, the development of Hollow Core optical fibers (HCs) [1, 2] is still very active. In particular, the use of hollow fiber structures comprising only a limited number of detached glass tubes within an outer glass jacket is gaining significant interest [3, 4]. The use of this fiber type has resulted in HCs with relatively low attenuation in the visible [5, 6], near [7, 8, 9] and mid-infrared spectral ranges [4], combined with ultra-large transmission bandwidths [5, 8, 9]. Possible applications of these hollow Anti-Resonant Fibers (ARFs) range from high power laser delivery [7] to gas based laser sources [10] and telecommunications [9].

Several modifications of this basic fiber design have been proposed [5, 11-15] in order to further reduce their level of leakage loss or increase their birefringence. However, all of the previous designs and fabrication proposals have concerned ARFs made of a single material (typically silica even though other glass materials have also been considered [16, 17]). In this paper we seek to explore a novel form of this ARF type, by using, for the first time (to our knowledge), multiple materials for the fiber cladding. We numerically study the transmission properties of these Composite Material Anti-Resonant Fibers (CM-ARFs*)*, by correlating the composite material membrane properties to that of a "single equivalent membrane", with an identical effective thickness and refractive index. We apply this concept to the design of a novel form of antiresonant fiber by adopting a hybrid semiconductor/glass core boundary membrane. Similarly to previous works on semiconductor optical fibers [18, 19], the inclusion of a semiconductor is desirable in order to realize functionalized devices. For example, a light induce refractive index change may be adopted for all optical fiber modulation [20]. We numerically demonstrate that, in contrast to previous structures with silicon in the cladding area [18], this novel type of Silicon Anti-Resonant Fiber is predicted to have very low attenuation (<0.1dB/m). Finally, we report on the first fabrication and characterization of a silicon/borosilicate based ARF.

Fig. 1 shows a reproduction of a silica based ARF (n=1.41 at λ=2.7μm) already fabricated in [4] with 10 cladding tubes and an original thickness of the cladding tubes t=2.4μm (in white). The core radius is 47μm. An additional internal membrane t_A (in red) is added corresponding to a material with refractive index n_2=2.

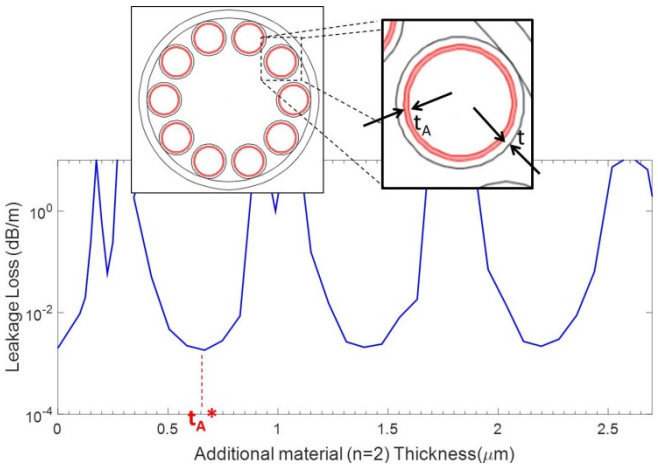

Fig. 1. Sketch (top) of a Composite Material Hollow Anti-resonant Fiber: an additional layer with thickness t_A is added to the original core boundary of thickness t. The fiber transmission spectrum at 2.7μm shows the anti-resonant behavior of the fiber.

The dependence of leakage loss on the additional thickness t_A shown in Fig.1 at a wavelength of 2.7µm, clearly demonstrates the anti-resonant properties of this CM-ARF. In the following, we will refer to an "antiresonant layer" as that additional membrane with a thickness t_A^* corresponding to the minimum leakage loss of the single layer ARF (see Fig. 1).

Fig. 2(a) shows the evolution of the leakage loss when additional antiresonant glass membranes (2, 3 or 5t) are added to the basic structure.

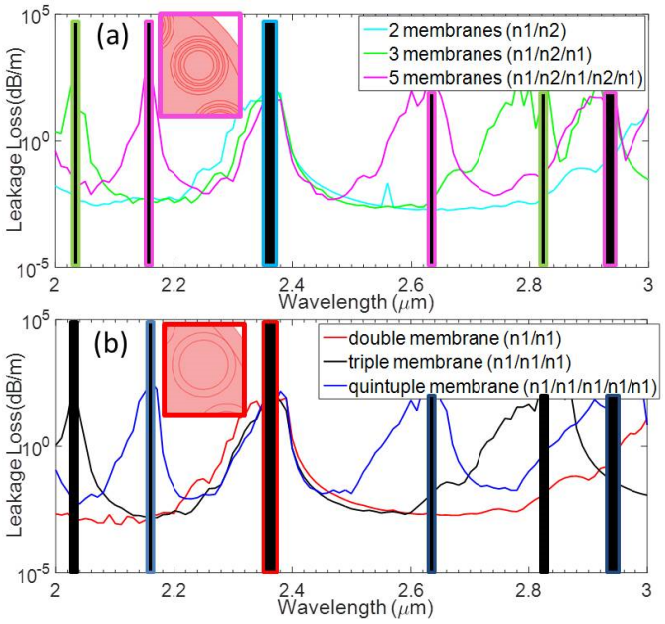

Fig. 2. Top (a): Calculated leakage loss when 2 (cyan line), 3 (green line) or 5 (pink line) antiresonant layers are added to the basic structure of Fig. 1. Bottom (b): Calculated leakage loss when the thickness t of the basic ARF structure is increased 2 (*2t*, red line), 3 (*3t*, black line) and 5 (*5t*, blue line) times.

This behavior is almost identical to that of fiber designs shown in Fig. 2(b) where the thickness of the initial single silica membrane is simply increased 2, 3 or 5 times (red, black and blue curve). In particular the fiber designs of (a) and (b) have the same resonant wavelengths and the same minimum leakage level. This is not surprising since the designs of Fig. 2(b) can be simply seen as multiple layers (of the type (a)) with the same refractive index for the alternating layers (n_2=n_1). By using the basic formulation of the resonant wavelength [21] it is possible to derive that the frequency spacing Δf between two resonant frequencies is

$$\Delta f = \frac{c}{2t_R\sqrt{n_1^2 - 1}} \qquad (1)$$

where c is the speed of light in vacuum, t_R is the membrane thickness of the ARF and n_1 is the glass refractive index. Therefore when the thickness is doubled or tripled the frequency spacing between two resonant frequencies is reduced by a factor of 2 or 3. This explains the presence in Fig. 2 of a different number of resonant wavelengths associated with the different number of antiresonant layers in the considered structures. The small differences between the spectra of Fig. 2(a) and (b) are only associated to the different optical coupling between the fundamental-like modes transmitted in the fiber core and the different cladding modes present in the two structures [8].

We can further extend the analogy between Fig. 2 (a) and (b) by correlating the behavior of a CM-ARF made of two materials (with refractive index n_1 and n_2, and thickness t_1 and t_2) to that of a single material ARF with an equivalent refractive index n_{eq} and thickness t_{eq}. We define:

$$n_{eq} = n_1\frac{S_1}{S_1 + S_2} + n_2\frac{S_2}{S_1 + S_2} \qquad (2)$$

and

$$t_{eq} = t_1 + t_2 \qquad (3)$$

where S_1 and S_2 are the surfaces occupied by the two materials and are given by (see inset of Fig. 3):

$$S_1 = \pi(r^2 - {r_1}^2) \qquad (4)$$

$$S_2 = \pi({r_1}^2 - {r_2}^2) \qquad (5)$$

where r_1 and r_2 are the internal radius of the two cladding tubes of thickness t_1 and t_2 respectively and r is the external radius of the composite material cladding tubes (see inset of Fig. 3). As an example and validation of this equivalence, we have considered the case of 2 materials with n_1=1.414 and n_2=2 (t_1=0.66µm, t_2=0.99 µm, r=20 µm). By using Eqns. 2 to 5 it is possible to obtain n_{eq}=1.7656 and t_{eq}=1.65 µm. By looking at Fig. 3 we can see that the leakage loss of the CM-ARF (blue line) and the equivalent ARF (red line) overlap in most of the considered spectral range. A slight difference between the two spectra is more evident at longer wavelengths where the fundamental mode interacts more strongly with the fiber cladding modes. The behavior of the equivalent structure is the same even when the fiber is bent with a bend radius greater than 10cm.

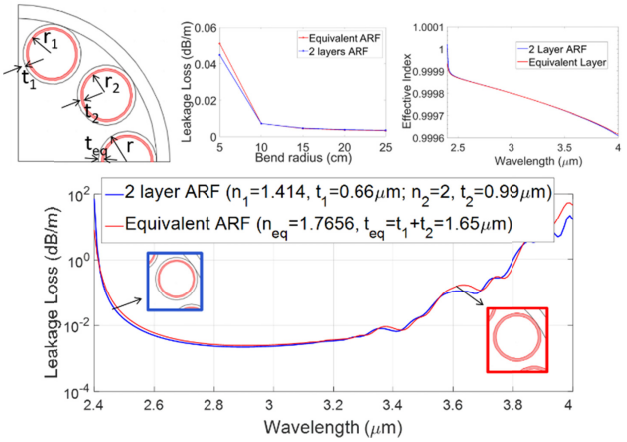

Fig. 3. Equivalence between a CM-ARF with 2 antiresonant layers of thickness t_1 and t_2 (blue line) and single layer ARF with an equivalent antiresonant layer of thickness t_{eq}.

The established analogy between a composite material and a conventional single material ARF suggests that only the overall optical path travelled by light at the core boundary is relevant for antiresonance guidance. This opens up the possibility to exploit the properties of additional materials deposited on the basic optical fiber matrix in order to activate and functionalize its behavior, for example, via the free carrier plasma-dispersion effect, in which the change of refractive index and absorption resulting from a change in the concentration of free carriers by photo-excitation can be used in silicon-based all-fibre integrated modulators to achieve intensity or phase modulation [20]. As a first step of this "active hollow core waveguide" concept, we have investigated the feasibility of a particular form of CM-ARF, in which the core boundary membrane is made of a composite hybrid semiconductor/glass material. Semiconductor optical fibers [19] have received great attention in the recent years because of the prospective for integration of the existing optical fibre infrastructure with the novel silicon photonics platform [22]. Since the first inclusions of semiconductors within optical fibres [23] progress in the area has seen some demonstrations of optical devices [19]. Although potentially these structures may provide unique characteristics, their use is currently limited by the very high attenuation observed to date in these fibres (of order 1dB/cm). Here we show that this problem can be mitigated by filling semiconductors within ARFs. Fig. 4 shows a typical section of a borosilicate based ARF [17] filled with amorphous hydrogenated silicon (a-Si:H) by using a High Pressure Chemical Vapor Deposition (HPCVD) method [23].

The CM-ARF of Fig. 4 (a) was obtained after a deposition of 48 hours at a temperature of 400 °C and has 3 layers of material (Silicon (white)/Borosilicate (gray)/Silicon (white). The Si layer thickness was measured using the SEM to be close to 300nm.

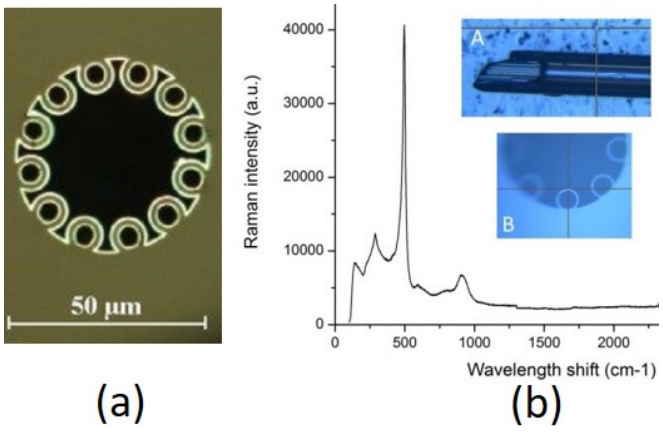

Fig. 4. (a) Fabricated CM-ARF: a thin (~0.3µm) layer of a:Si-H (highly reflective white material) covers the internal and external sides of the cladding tubes of a borosilicate based ARF. (b) Raman Shift spectrum of another CM-ARF shown in its longitudinal (A) and transversal (B) section. The peaks reveal the presence of a-Si:H on the external and internal surfaces of the cladding tubes. Reflective white material (a-Si:H) can also be seen in the longitudinal section (A) micrograph.

We then tested several types of ARF by using the same HPCVD technique and modifying the temperature profile along the fiber samples as well as the filling time. The fiber shown in the inset of Fig. 4(b) (core diameter *d*=60µm and glass layer thickness of 1µm) was coiled in a furnace at a temperature of 450 °C and filled for only 4 hours in order to obtain a very thin a-Si:H layer thickness. A length of 35 cm of this fibre was obtained and tested.

We could reveal the presence of a thin layer of a-Si:H by means of Raman Spectroscopy. Figure 4(b) shows the Raman Shift spectrum taken using the sample in the inset (shown in its longitudinal section (A) and transversal section (B)) and using an optical pump at a wavelength of 0.63 µm. The Raman shift at the points centred on the external and internal side of the cladding tubes confirm the presence of a-Si:H [24].

The spectrum of the signal transmitted through the considered 35cm long sample is shown in Fig. 5 together with the near field intensity profile recorded by an Infrared Camera. In the considered spectral range (0.7µm to 1.6 µm) the CM-ARF has two transmission windows (just above 0.8 µm and around 1.2 µm) and presents several peaks probably related to the coupling of the fundamental-like mode (in the inset) to the cladding modes, in both the high refractive index (~3.6) of the a-Si:H.

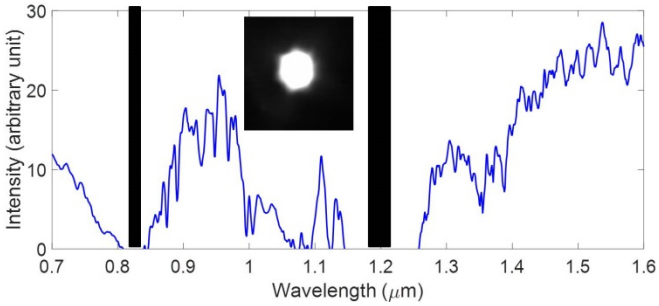

Fig. 5. Transmission spectrum of the CM-ARF shown in the inset of Fig. 4 (b) and Fig. 7. Inset: near field intensity profile of the transmitted optical mode.

In Fig. 6(A) we have compared this measured transmission spectrum (blue solid line) with that of 7 meters of the same ARF without any silicon filling (green solid line, glass thickness is 1µm and glass dispersion is taken into account) and the calculation of the leakage loss for both the filled CM-ARF (black dotted line) and the unfilled ARF (red dotted line). Our simulations show how the addition of the internal and external silicon layer to the original ARF results in a red-frequency shift of the entire transmission spectrum. Fig. 6(B) shows what would be the effect on the leakage loss of a variation of the coating thickness of ±10nm, proving that the fiber attenuation levels would be kept similar but there would be a shift of the resonant wavelength (±0.05µm).

In order to show the impact of the optical absorption of the a-Si:H layers on the fibre performance we have compared in Fig. 7 the attenuation components of the CM-ARF. The fiber attenuation related to the presence of a glass (red line) and silicon (green line) material absorption are obtained as the product between the optical mode overlap on each material and their intrinsic absorption. Concerning this last quantity, we have measured the

borosilicate glass absorption to be maximum 140dB/m and we have assumed a high absorption of the amorphous silicon material of 100dB/cm.

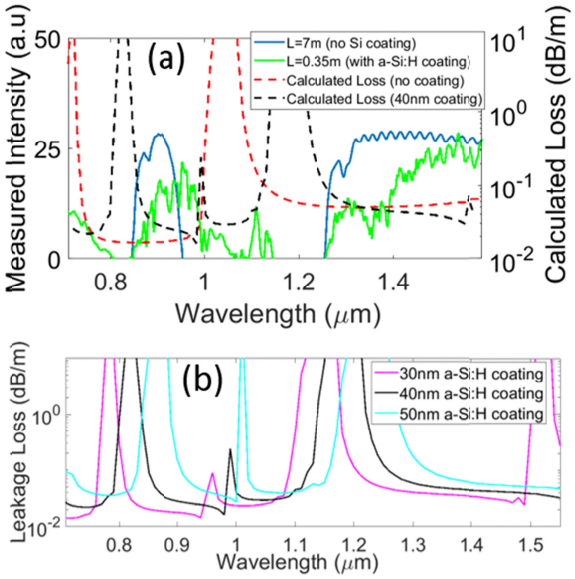

Fig. 6(a) Comparison between the transmission spectrum (left Y axis) of an unfilled ARF (7m long, green solid line) and the same ARF filled with a-SI:H (0.35m long, blue solid line) with the calculated leakage loss (right Y axis) of the unfilled ARF (red dotted line) and the a-Si-H filled ARF (40nm coating, black dotted line).(b)Calculated leakage loss for 30,40 and 50 nm coating thickness.

The results show that, for the considered fiber, the leakage loss (blue line) is the most important contribution to the total attenuation of the CM-ARF and demonstrates the negligible impact of the absorption of the deposited semiconductor. As shown in Fig. 7, levels of attenuation as low as 0.1dB/m or less may be obtainable in long CM-ARFs.

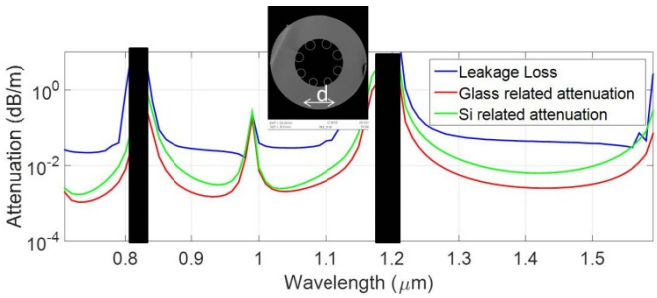

Fig. 7. Different components of the total attenuation of the CM-ARF shown in the inset: leakage loss (blue line), loss related to the overlap of the optical mode on the Si layer (green line) and on the borosilicate cladding layer (red line). The material absorption has been assumed to be 10000dB/m for a-Si:H and 140dB/m for borosilicate.

In conclusion, in this work we have demonstrated that CM-ARFs have the same characteristics of single layer ARFs. We have formulated an equivalence between single layer and CM-ARFs. By using this concept, we have fabricated and characterized the first silicon based ARF, showing the potential of this platform for the realization of semiconductor based devices with low attenuation. The exploration of this new avenue of research may lead to the implementations of novel forms of composite (glass/semiconductor) devices based on hollow core optical fiber technology with intriguing prospects in the broad fields of optical sensing, communications, light generation and manipulation.

Funding. EPSRC (EP/I035307/1 and EP/I01196X/1). Datasets at http://doi.org/10.5258/SOTON/D0046

References

1. R. F. Cregan, B. J. Mangan, J. C. Knight, T. A. Birks, and P. St. J. Russell, Science 285(1999).
2. P. J. Roberts, F. Couny, H. Sabert, B. J. Mangan, D. P. Williams, L. Farr, M. W. Mason, A. Tomlinson, T. A. Birks, J. C. Knight and P. St. J. Russell, Opt. Express 13, (2005).
3. A. N. Kolyadin, A. F. Kosolapov, A. D. Pryamikov, A. S. Biriukov, V. G. Plotnichenko, and E. M. Dianov, Opt. Express 21, 9514-9519 (2013).
4. W. Belardi and J. C. Knight, Opt. Express 22, 10091-10096 (2014).
5. W. Belardi, *J. Lightwave Technology*, vol. 33, 4497-4503 (2015).
6. S. Gao, Y. Wang, X. Liu, C. Hong, S. Gu, and P. Wang" Opt. Lett. 42, 61-64 (2017).
7. M. Michieletto, J. K. Lyngsø, C. Jakobsen, J. Lægsgaard, O. Bang, and T. T. Alkeskjold, Opt. Express 24, 7103-7119 (2016).
8. B. Debord, A. Amsanpally, M. Chafer, A. Baz, M. Maurel, J. M. Blondy, E. Hugonnot, F. Scol, L. Vincetti, F. Gérôme, and F. Benabid, Optica 4, 209-217 (2017).
9. J. R. Hayes, S. R. Sandoghchi, T. D. Bradley, Z. Liu, R. Slavik, M. A. Gouveia, N. V. Wheeler, G. T. Jasion, Y. Chen, E. Numkam-Fokoua, M. N. Petrovich, D. J. Richardson, and F. Poletti,, *OFC 2016*, Th5A.3.
10. Z. Wang, W. Belardi, F. Yu, W. J. Wadsworth, and J. C. Knight, Opt. Express 22, 21872-21878 (2014).
11. W. Belardi and J. C. Knight, *OFC 2014*, Th2A.45 (Supplementary Material)
12. Md. S. Habib, O. Bang, and M. Bache, Opt. Express 24, 8429-8436 (2016).
13. X. Huang, W. Qi, D. Ho, K. Yong, F. Luan, and S. Yoo, Opt. Express 24, 7670-7678 (2016).
14. Md I. Hasan, N. Akhmediev, and W. Chang Opt. Lett.42, 703-706 (2017).
15. W. Ding and Y. Wang, Opt. Express 23, 21165-21174 (2015).
16. A. F. Kosolapov, A. D. Pryamikov, A. S. Biriukov, V. S. Shiryaev, M. S. Astapovich, G. E. Snopatin, V. G. Plotnichenko, M. F. Churbanov, and E. M. Dianov, Opt. Express 19, 25723-25728 (2011).
17. W. Belardi, N. White, J. Lousteau, X. Feng, and F. Poletti, *WSOF 2015*, WW4A.4.
18. N. Healy, J. R. Sparks, R. R. He, P. J. A. Sazio, J. V. Badding, and A. C. Peacock, Opt. Express 19, 10979-10985 (2011).
19. J. R. Sparks, P. J. A. Sazio, V. Gopalan and J. V. Badding, Annu. Rev. Mater. Res. 43, 527 (2013).
20. D. Won, M. O. Ramirez, H. Kang, V. G. F. Baril, J. Calkins, J V. Badding, P. J. A. Sazio, Appl. Phys. Lett. 91, 161112 (2007)
21. N. M. Litchinitser, A. K. Abeeluck, C. Headley, and B. J. Eggleton, Opt. Lett. 27(18),1592-1594 (2002).
22. D. Thomson, A. Zilkie, J. E Bowers, T. Komljenovic, G. T Reed, L. Vivien, D. Marris-Morini, E. Cassan, L. Virot, J. Fédéli, J. Hartmann,J. H Schmid, D. Xu, F. Boeuf, P. O'Brien, G. Z. Mashanovich and M Nedeljkovic, J. of Optics, 18, 073003 (2016).
23. P. J. .Sazio, A. .Amezcua-Correa, C.. E. .Finlayson, J. R. Hayes, T. .J. Scheidemantel, N. F. Baril, B. R. Jackson, D. J.Won, F. Zhang, E.. R. Margine, V. Gopalan, V. H. Crespi, J. V. Badding, *Science* 311, 1583-1586 (2006).
24. V. A. Volodin and D. I. Koshelev, J. Raman Spectrosc., 44, 1760–1764 (2013).

References

1. R. F. Cregan, B. J. Mangan, J. C. Knight, T. A. Birks, and P. St. J. Russell," Single-Mode Photonic Band Gap Guidance of Light in Air" Science 285, 1537 (1999).
2. P. J. Roberts, F. Couny, H. Sabert, B. J. Mangan, D. P. Williams, L. Farr, M. W. Mason, A. Tomlinson, T. A. Birks, J. C. Knight and P. St. J. Russell, "Ultimate low loss of hollow-core photonic crystal fibres," Opt. Express 13, 236-244 (2005).
3. A. N. Kolyadin, A. F. Kosolapov, A. D. Pryamikov, A. S. Biriukov, V. G. Plotnichenko, and E. M. Dianov, "Light transmission in negative curvature hollow core fiber in extremely high material loss region," Opt. Express 21(8), 9514-9519 (2013).
4. W. Belardi and J. C. Knight, "Hollow antiresonant fibers with low bending loss", Opt. Express 22, 10091-10096 (2014).
5. W. Belardi, "Desig and properties of hollow antiresonant fibers for the visible and near infrared spectral range" *J. Lightwave Technology*, vol. 33, no. 21, pp. 4497-4503 (2015)
6. Shou-fei Gao, Ying-ying Wang, Xiao-lu Liu, Chang Hong, Shuai Gu, and Pu Wang, "Nodeless hollow-core fiber for the visible spectral range," Opt. Lett. 42, 61-64 (2017)
7. M. Michieletto, J. K. Lyngsø, C. Jakobsen, J. Lægsgaard, O. Bang, and T. T. Alkeskjold, "Hollow-core fibers for high power pulse delivery," Opt. Express 24, 7103-7119 (2016)
8. B. Debord, A. Amsanpally, M. Chafer, A. Baz, M. Maurel, J. M. Blondy, E. Hugonnot, F. Scol, L. Vincetti, F. Gérôme, and F. Benabid, "Ultralow transmission loss in inhibited-coupling guiding hollow fibers," Optica 4, 209-217 (2017)
9. J. R. Hayes, S. R. Sandoghchi, T. D. Bradley, Z. Liu, R. Slavik, M. A. Gouveia, N. V. Wheeler, G. T. Jasion, Y. Chen, E. Numkam-Fokoua, M. N. Petrovich, D. J. Richardson, and F. Poletti, "Antiresonant Hollow Core Fiber with Octave Spanning Bandwidth for Short Haul Data Communications," in *OFC 2016*, paper Th5A.3.
10. Z. Wang, W. Belardi, F. Yu, W. J. Wadsworth, and J. C. Knight, "Efficient diode-pumped mid-infrared emission from acetylene-filled hollow-core fiber," Opt. Express 22, 21872-21878 (2014)
11. W. Belardi and J. C. Knight, "Negative curvature fibers with reduced leakage loss", *OFC 2014*, paper Th2A.45 (Supplementary Material)
12. Md. S. Habib, O. Bang, and M. Bache, "Low-loss single-mode hollow-core fiber with anisotropic anti-resonant elements," Opt. Express 24, 8429-8436 (2016)
13. X. Huang, W. Qi, D. Ho, K. Yong, F. Luan, and S. Yoo, "Hollow core anti-resonant fiber with split cladding," Opt. Express 24, 7670-7678 (2016)
14. Md I. Hasan, N. Akhmediev, and W. Chang, "Positive and negative curvatures nested in an antiresonant hollow-core fiber," Opt. Lett.42, 703-706 (2017)
15. W. Ding and Y. Wang, "Hybrid transmission bands and large birefringence in hollow-core anti-resonant fibers," Opt. Express 23, 21165-21174 (2015)
16. A. F. Kosolapov, A. D. Pryamikov, A. S. Biriukov, V. S. Shiryaev, M. S. Astapovich, G. E. Snopatin, V. G. Plotnichenko, M. F. Churbanov, and E. M. Dianov, "Demonstration of CO_2-laser power delivery through chalcogenide-glass fiber with negative-curvature hollow core," Opt. Express 19, 25723-25728 (2011)
17. W. Belardi, N. White, J. Lousteau, X. Feng, and F. Poletti, "Hollow Core Antiresonant Fibers in Borosilicate Glass," in *WSOF 2015*, paper WW4A.4.
18. N. Healy, J. R. Sparks, R. R. He, P. J. A. Sazio, J. V. Badding, and A. C. Peacock, "High index contrast semiconductor ARROW and hybrid ARROW fibers," Opt. Express 19, 10979-10985 (2011)
19. J. R. Sparks, P. J. A. Sazio, V. Gopalan and J. V. Badding, Annu. Rev. Mater. Res., "Templated chemically deposited semiconductor optical fiber materials", 43, 527 (2013).
20. D. Won, M. O. Ramirez, H. Kang, V. G. F. Baril, J. Calkins, J V. Badding, P. J. A. Sazio, "All-optical modulation of laser light in amorphous silicon-filled microstructured optical fibers", Appl. Phys. Lett. 91, 161112 (2007)
21. N. M. Litchinitser, A. K. Abeeluck, C. Headley, and B. J. Eggleton,"Antiresonant reflecting photonic crystal optical waveguides," Opt. Lett. 27(18),1592-1594 (2002).
22. D. Thomson, A. Zilkie, J. E Bowers, T. Komljenovic, G. T Reed, L. Vivien, D. Marris-Morini, E. Cassan, L. Virot, J. Fédéli, J. Hartmann,J. H Schmid, D. Xu, F. Boeuf, P. O'Brien, G. Z. Mashanovich and M Nedeljkovic, "Roadmap on silicon photonics", J. of Optics, 18(7), 073003 (2016).
23. P. J. A.Sazio, A. Amezcua-Correa, C. E. Finlayson, J. R. Hayes, T. J. Scheidemantel, N. F. Baril, B. R. Jackson, D. J. Won, F. Zhang, E.R.Margine, V.Gopalan, V.H.Crespi, J.V.Badding, "Microstructured optical fibers as high-pressure microfluidic reactors" *Science* 311(5767) 1583-1586 (2006)
24. V. A. Volodin and D. I. Koshelev, "Quantitative analysis of hydrogen in amorphous silicon using Raman scattering spectroscopy", J. Raman Spectrosc., 44, 1760–1764 (2013)